Rare B Decays

Toru Iijima
Department of Physics, Nagoya University, Chikusa, Nagoya, 464-8602, Japan

This paper reviews recent experimental results for rare B meson decays, in view of searching for new physics effects, based on data collected by Belle and BaBar at the B-factories, as well as CDF and D0 at the Tevatron.

1 Introduction

The success of B factories, both at KEK and SLAC, have brought the quantitative confirmation of the theory proposed by Kobayashi-Maskawa to explain the CP violation [1]. So far, all the measurements, relevant to the three internal angles and three sides of the Unitarity Triangle (UT), are consistent. It indicates that there is no $O(1)$ correction from New Physics (NP), however, there is still room for sub-leading contribution at $O(0.1)$. Decays of the B meson, the heaviest meson containing the third generation quark, involve a variety of Feynman diagrams sensitive to NP, such as penguin, box and annihilation diagrams. This paper reviews the present status of NP search in the following categories; a) B decays with missing energy($b \to \tau\nu, c\tau\nu, b \to \ell\nu(\gamma)$), b) electromagnetic ($b \to s\gamma$) and electroweak ($b \to s\ell\ell$) penguins, c) leptonic decays ($B_{s(d)} \to \ell\ell$) and d) gluonic penguin decays ($b \to sg$ and $b \to uq\bar{q}$). Relevant Feynman diagrams are shown in Figure 1. Results are taken from Belle and BaBar at the B factories, as well as CDF and D0 at the Tevatron. Throughout the paper, charge conjugate states are implied, and the first and second errors in numerical results represent statistical and systematic errors, respectively.

Studies of rare B decays, especially at the B-factories, rely on success of the accelerators. Figure 2 shows the integrated luminosity of the two experiments, KEKB/Belle and PEP II/BaBar. The achieved peak luminosity is $2.1 \times 10^{34}\text{cm}^{-2}\text{s}^{-1}$ for KEKB and $1.2 \times 10^{34}\text{cm}^{-2}\text{s}^{-1}$ for PEP II. The number of produced $B\overline{B}$ pairs exceeds 800 million for Belle and 470 million for BaBar. Such high luminosity data have enabled us not only to observe rare B decay modes but also to measure detailed information, i.e., distribution of decay quantities, such as decay angle, q^2 and so on.

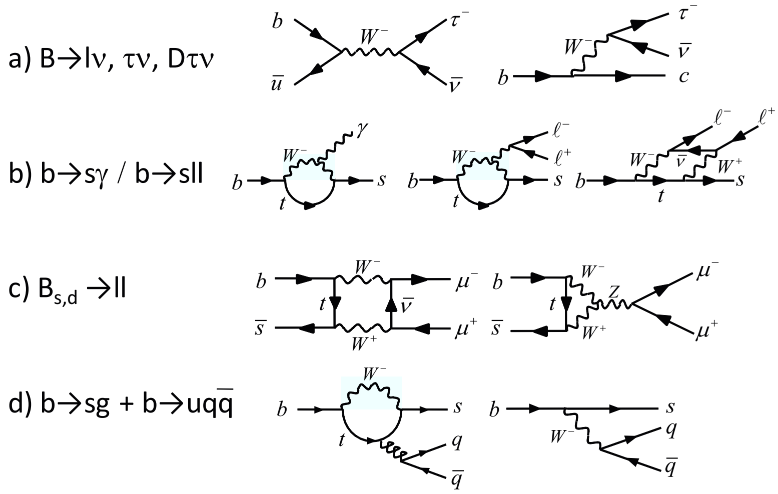

Figure 1: Feynman diagrams of rare B decays discussed in this paper.

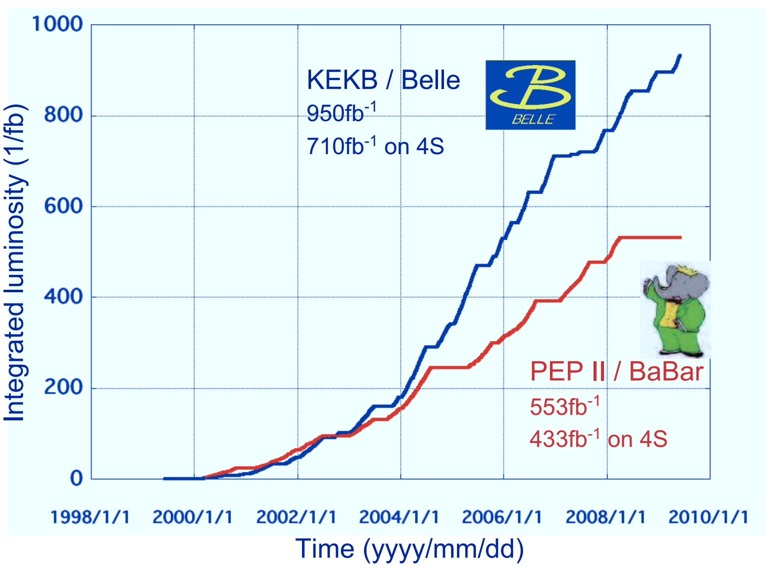

Figure 2: Integrated luminosity at the B factories.

2 B Decays with Missing Energy ($B \to \tau\nu, D\tau\nu, \ell\nu(\gamma)$)

2.1 $B \to \tau\nu$

In the Standard Model (SM), the purely leptonic decay $B^- \to \tau^-\bar{\nu}$ proceeds via annihilation of b and $\overline{u}$ quarks to a W^- boson (see Figure 1). The branching fraction is given by

$$\mathcal{B}(B^- \to \tau^-\bar{\nu}) = \frac{G_F^2 m_B m_\tau^2}{8\pi}\left(1 - \frac{m_\tau^2}{m_B^2}\right)^2 f_B^2 |V_{ub}|^2 \tau_B, \tag{1}$$

where G_F is the Fermi coupling constant, m_B and m_τ are the B and τ masses, respectively, and τ_B is the B^- lifetime [2]. The expected branching fraction is $(1.20 \pm 0.25) \times 10^{-4}$ using $|V_{ub}| = (4.32 \pm 0.33) \times 10^{-3}$, determined by inclusive charmless semileptonic B decay data [3], and $f_B = 0.190 \pm 0.013$ GeV obtained from recent lattice QCD calculations [4]. Physics beyond the SM, such as supersymmetry or two-Higgs doublet models, could modify $\mathcal{B}(B^- \to \tau^-\bar{\nu})$ through the introduction of a charged Higgs boson [5]. The charged Higgs boson effect is given by $\mathcal{B}(B^- \to \tau^-\bar{\nu}) = \mathcal{B}(B^- \to \tau^-\bar{\nu})_{SM} \times r_H$, where the ratio r_H is given by $r_H = (1 - m_B \tan^2\beta / m_{H^\pm})^2$, using the charged Higgs mass $m_{H^\pm}$ and the ratio of the two Higgs vacuum expectation values $\tan\beta$.

Experimentally, it is challenging to detect decay modes including neutrinos in the final state, such as $B \to \tau\nu$ and $B \to D\tau\nu$ discussed in the following sub-section, since they cannot be kinematically constrained. In order to suppress background, the accompanying B mesons are reconstructed, by using hadronic decays, by using semileptonic decays, and also by calculating the four-vector sum of the PID tracks inclusively without reconstructing the intermediate mesons. Then, on the other side, signals are identified by detecting charged tracks from the signal decays, requiring no extra activities in the electro-magnetic calorimeter, and calculating the missing energy due to neutrinos.

Both Belle and BaBar collaborations have reported branching fractions using the hadronic and semileptonic tags, as summarized in Table 1. Figure 3-a) shows distributions of the extra energy in the electromagnetic colorimeter on the signal side ($E_{\rm ECL}$), reported by Belle using the semileptonic tags, where one can see the excess due to $B \to \tau\nu$ signals near $E_{\rm ECL} = 0$. The naive average branching fraction is calculated to be $\mathcal{B}(B \to \tau\nu)_{AVG} = (1.73 \pm 0.35) \times 10^{-4}$, which is consistent with the above SM prediction, and leads to the ratio $r_H = 0.95 \pm 0.32$. Based on this result, the charged Higgs can be constrained in the $(\tan\beta, m_H)$ plane, as shown in Figure 3-b).

It should be noted here that there appears tension in this comparison, if the SM value is taken from the CKM fit rather than from Eq.(1) with inputs of f_B and $|V_{ub}|$. In this case, the average branching fraction $\mathcal{B}(B \to \tau\nu)_{AVG}$ is 2.4 σ higher than the prediction, $\mathcal{B}(B \to \tau\nu)_{\rm CKMfit} = (0.786^{+0.179}_{-0.083}) \times 10^{-4}$.

2.2 $B \to D\tau\nu$

The semileptonic B decay to the τ channel, $B \to D^{(*)}\tau\nu$, is also sensitive to the charged Higgs. In the SM, the decay occurs via an external W emission diagram with predicted branching fractions of $(0.69 \pm 0.04)\%$ and $(1.41 \pm 0.07)\%$ for $B^0 \to D^-\tau^+\nu_\tau$ and $B^0 \to D^{*-}\tau^+\nu_\tau$, respectively [10]. On the other hand, if a charged Higgs boson ($H^\pm$) exists, it contributes to the decay amplitude at tree level, and the branching fraction can be modified significantly [11]. The charged Higgs can be constrained based on the ratio, $R(D) = \mathcal{B}(B \to D\tau\nu)/\mathcal{B}(B \to D\ell\nu)$.

Exp.	Tag	$N_{B\bar{B}}$ (10^6)	B (10^{-4})	Ref.
Belle	hadronic	449	$1.79^{+0.56+0.46}_{-0.49-0.51}$	[6]
Belle	semileptonic	657	$1.65^{+0.38+0.35}_{-0.37-0.37}$	[7]
BaBar	hadronic	383	$1.8^{+0.9}_{-0.8} \pm 0.4 \pm 0.2$	[8]
BaBar	semileptonic	459	$1.8 \pm 0.8 \pm 0.1$	[9]
Average			1.73 ± 0.35	

Table 1: Measured branching fractions for $B^- \to \tau^- \bar{\nu}$.

The $B \to D^{(*)}\tau\nu$ and $B^+ \to \tau^+\nu_\tau$ decays have similar sensitivity to $H^\pm$, but with different theoretical systematics; the former suffers from uncertainty in the form factor, while the latter requires knowledge of the B decay constant f_B. Therefore, they provide complementary approaches to searching for $H^\pm$ signatures in B decays.

The BaBar collaboration presented the first evidence of the $B \to D\tau\nu$ decay, by applying the hadronic tags to the 238M $B\bar{B}$ sample. As shown in Figure 3-c), both $B \to D\tau\nu$ and $B \to D^*\tau\nu$ signals are seen as excess of events in the large missing mass region [12]. When D^0 and D^+ modes are combined, the significance of the $B \to D\tau\nu$ signal is found to be 3.6σ, including systematics, and the ratio is found to be $R(D) = 0.42 \pm 0.12 \pm 0.05$. The Belle collaboration applied the inclusive tags, and reported the first observation of $B \to D^*\tau\nu$ [13]. More recently, they has reported preliminary results of $B \to D^{(*)}\tau\nu$ by using the hadronic tag methods, and obtained $R(D) = 0.60 \pm 0.14 \pm 0.08$ [14]. The naive average of the BaBar and Belle results for the ratio is found to be $R(D) = 0.49 \pm 0.10$. This provides a constraint on the charged Higgs, comparable to the one obtained by $B \to \tau\nu$, as shown in Figure 3.

2.3 $B \to \ell\nu(\gamma)$

The BaBar collaboration has presented results of search for purely leponic decays in the electron and muon channels, by applying the inclusive tags on the 468 M $B\bar{B}$ data set. [15]. Reported upper limits for the muon channel, $\mathcal{B}(B \to \mu\nu) < 1.0 \times 10^{-6}$ (90% C.L.), is about a factor of 2 larger than the SM value. They have also reported upper limits for the radiative leptonic decays [16].

3 Radiative Penguin Decays ($b \to s\gamma$)

The radiative penguin decay is one of the most powerful tool to constrain NP. The large data sample at the B factories enable us to measure not only the branching fractions, but also more detailed information such as isospin asymmetry, direct CP asymmetry, as well as the mixing induced time-dependent CP violation. The photon energy spectrum is also an ideal tool to determine the HQE parameters, which are required in deducing $|V_{cb}|$ and $|V_{nb}|$ from semileptonic B decays.

3.1 Exclusive $B \to X_s\gamma$

Figure 4-a) shows the new measurements of exclusive $B \to K^*(892)\gamma$ decays by BaBar, based on 383 M $B\bar{B}$ sample [17]. The figures demonstrate how precisely these decays are measured in the

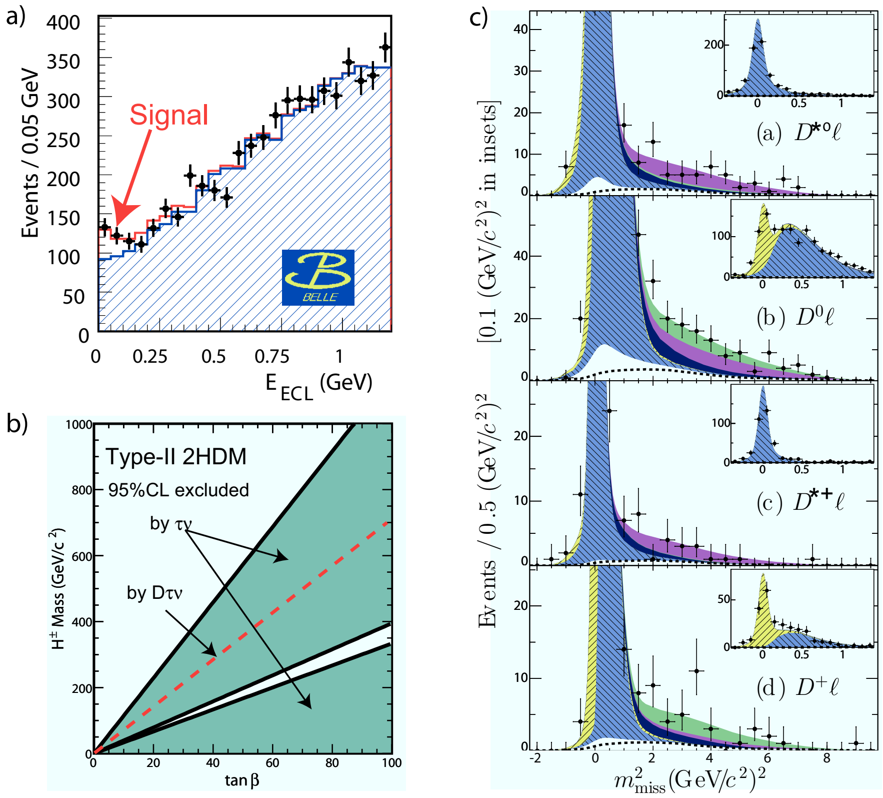

Figure 3: a) Distribution of residual energy E_{ECL} reported by Belle using semileptonic tags. $B^- \to \tau^- \bar{\nu}$ signals are seen near $E_{ECL} = 0$. b) Constraint on charged Higgs in the $(\tan\beta, m_H)$ plane in the type-II two Higgs doublet models. Hatched regions are excluded by $B \to \tau\nu$ at 95% confidence level. The similar exclusion limit by $B \to D\tau\nu$ is also shown by the dashed line. c) Distribution of the missing mass squared $m^2_{\rm miss}$ reported by BaBar using hadronic tags. $B \to D^{(*)}\tau\nu$ signals are seen in the large $m^2_{\rm miss}$ region.

B-factory era. The reported branching fractions are, $\mathcal{B}(B^0 \to K^{*0}\gamma) = (4.47 \pm 0.10 \pm 0.16) \times 10^{-5}$ and $\mathcal{B}(B^+ \to K^{*+}\gamma) = (4.22 \pm 0.14 \pm 0.16) \times 10^{-5}$, which lead to the isospin asymmetry,

$$\Delta_{0+}(B \to K^*\gamma) = \frac{\Gamma(\overline{B}^0 \to \overline{K}^{*0}\gamma) - \Gamma(B^- \to K^{*-}\gamma)}{\Gamma(\overline{B}^0 \to \overline{K}^{*0}\gamma) + \Gamma(B^- \to K^{*-}\gamma)} = 0.066 \pm 0.021 \pm 0.022 \ . \qquad (2)$$

The result is consistent with the SM value $(2 - 10\%)$. They have also reported the direct CP asymmetry, $A_{CP}(B \to K^*\gamma) = -0.003 \pm 0.017 \pm 0.007$, and it is consistent with the SM value $(\sim 1\%)$.

The mixing-induced time-dependent CP violation in $b \to s\gamma$ processes is of particular interest as a sensitive probe to unknown right-handed currents. In the SM, photon polarization is flavor specific, and CPV is not expected. On the other hand, if non-SM right-handed current exists, CP violation may appear. The BaBar collaboration has reported such a measurement using the $B \to K\eta\gamma$ decay, based on the full data set (484M $B\overline{B}$) [18]. The reported results are, $\mathcal{B}(B^0 \to K^0_S\eta\gamma) = (7.1^{+2.1}_{-2.0} \pm 0.4) \times 10^{-6}, S_{K_S\eta\gamma} = -0.18^{+0.49}_{-0.46} \pm 0.12, C_{K_S\eta\gamma} = -0.32^{+0.40}_{-0.39} \pm 0.07$. They reported also the branching fraction and direct CP asymmetry for charged B decays, $\mathcal{B}(B^+ \to K^+\eta\gamma) = (7.7 \pm 1.0 \pm 0.4) \times 10^{-6}, A_{CP}(B^+ \to K^+\eta\gamma) = (-9.0^{10.4}_{-9.8} \pm 1.4) \times 10^{-2}$.

The Belle collaboration has reported the results of $B \to K\eta^{'}\gamma$ decay; evidence for the charged B mode, and upper limit for the neutral B, based on the 657M $B\overline{B}$ sample, $\mathcal{B}(B^+ \to K^+\eta^{'}\gamma) = (3.6 \pm 1.2 \pm 0.4) \times 10^{-6}(3.3\sigma)$, $\mathcal{B}(B^0 \to K^0\eta^{'}\gamma) < 6.4 \times 10^{-6}(90\%\text{C.L.})$. [19] They also observed $B \to K\phi\gamma$ decays, based on the 772M $B\overline{B}$ sample [20]. These decay modes will be used for time-dependent CP violation measurements in the near future.

3.2 Inclusive $B \to X_s\gamma$

The Belle collaboration has reported a new result for the inclusive $B \to X_s\gamma$ branching fraction, based on 657M $B\bar{B}$ sample [21]. In the new result, the photon energy threshold is lowered to $1.7\,\text{GeV}/c$, by which 97% of the decay phase space are covered. This leads to less systematic uncertainty when the result is extrapolated to the total branching fraction and compared to theoretical calculations. Two streams are used in the analysis; one is without tags (MAIN) and the other one with tags using leptons from B decays (LT), which is useful to suppress continuum background. Figure 4-b) shows the photon energy spectrum obtained by averaging the two results. The partial branching fraction in the photon energy range between 1.7 and 2.8GeV, is obtained as $\mathcal{B}(B \to X_s\gamma; 1.7 < E_\gamma(\text{GeV}) < 2.8) = (3.45 \pm 0.15 \pm 0.40) \times 10^{-4}$ with the systematic error dominated by uncertainty in the background estimation.

The new world average for the branching fraction above 1.6GeV is calculated to be $\mathcal{B}(B \to X_s\gamma; E_\gamma > 1.6GeV) = (3.57 \pm 0.24) \times 10^{-4}$, which shows marginal consistency with the most recent NNLO calculation, $(3.15 \pm 0.23) \times 10^{-4}$ [22]. The result constraints the charged Higgs mass above 300GeV. Search for charged Higgs in B decays, $B \to X_s\gamma$ as well as $B \to \tau\nu$ are complementary to the direct search at hadron colliders.

4 Electroweak Penguin Decays ($b \to s\ell\ell$)

The $b \to s\ell\ell$ decay proceeds via the electroweak penguin or box diagrams, to which NP can contribute significantly. There are many observables and distributions, which can be tested, such as the q^2 distribution, K^* longitudinal polarization (F_L), forward-backward asymmetry (A_{FB}), isospin asymmetry (A_I).

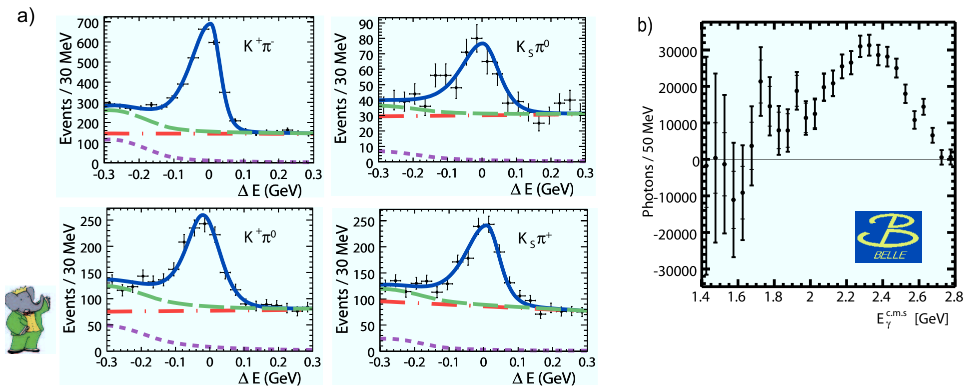

Figure 4: a) Updated results for the exclusive $B \to K^*(892)\gamma$ decays by BaBar. b) The photon energy spectrum for the $B \to X_s\gamma$ reported by Belle.

Table 2 summarized the branching fractions of exclusive $B \to K^*\ell\ell$ decays reported by the Belle, BaBar and CDF experiments. The average branching fraction is found to be $\mathcal{B}(B \to K^*\ell\ell) = (10.0 \pm 1.1) \times 10^{-7}$ and $\mathcal{B}(B \to K\ell\ell) = (4.3 \pm 0.4) \times 10^{-7}$. The q^2 distributions have also been measured, and they are found to be consistent with theoretical predictions within errors.

Exp.	$\mathcal{B}(B \to K^*\ell\ell)$ $[10^{-7}]$	$\mathcal{B}(B \to K\ell\ell)$ $[10^{-7}]$	Ref.
Belle	$10.7^{+1.1}_{-1.0} \pm 0.9$	$4.8^{+0.5}_{-0.4} \pm 0.3$	[23]
BaBar	$7.8^{+1.9}_{-1.7} \pm 1.1$	$3.4 \pm 0.7 \pm 0.2$	[24]
CDF	$8.1 \pm 3.0 \pm 1.0$	$5.9 \pm 1.5 \pm 0.4$	[25]
Average	10.0 ± 1.1	4.3 ± 0.4	

Table 2: Measured branching fractions for $B \to K^{(*)}\ell\ell$. Only $B \to K^{(*)}\mu\mu$ are measured in the CDF result.

The forward-backward asymmetry of the leptons from the $B \to K^*\ell\ell$ is generated by γ/Z interference, and is one of the most interesting observables to search for NP. In both Belle and BaBar analysis, in each q^2 bin, the K^* longitudinal polarization fraction (F_L) is measured by fitting the angular distribution of the kaon, and then the asymmetry (A_{FB}) is deduced by fitting the signal PDF, $\frac{3}{4}F_L(1-\cos^2\theta_{B\ell}) + \frac{3}{8}(1-F_L)(1+\cos^2\theta_{B\ell}) + A_{FB}\cos\theta_{B\ell}$, to the distribution of the angle between the lepton and B meson ($\theta_{B\ell}$). Figure 5 shows the obtained A_{FB} as a function of q^2, compared to the SM prediction shown by blue lines. In the Belle result, the obtained A_{FB} exceeds the SM with a 2.7 σ significance.

Another interesting observable is the isospin asymmetry, defined as,

$$A_I \equiv \frac{(\tau_{B^+}/\tau_{B^0}) \times \mathcal{B}(K^{(*)0}\ell^+\ell^-) - \mathcal{B}(K^{(*)\pm}\ell^+\ell^-)}{(\tau_{B^+}/\tau_{B^0}) \times \mathcal{B}(K^{(*)0}\ell^+\ell^-) + \mathcal{B}(K^{(*)\pm}\ell^+\ell^-)}. \quad (3)$$

As shown in Figure 6, data present slight negative deviation in the low q^2 region below the J/ψ

veto region. The deviation is more significant in the BaBar result; 2.7 σ and 3.2 σ away from zero for $K^*\ell\ell$ and $K\ell\ell$ mode, respectively, and 3.9 σ when the two modes are combined.

It is of particular interest to see the results for A_{FB} and A_I using the full data sets from the two B-factory experiments, and also from the Tevatron experiments.

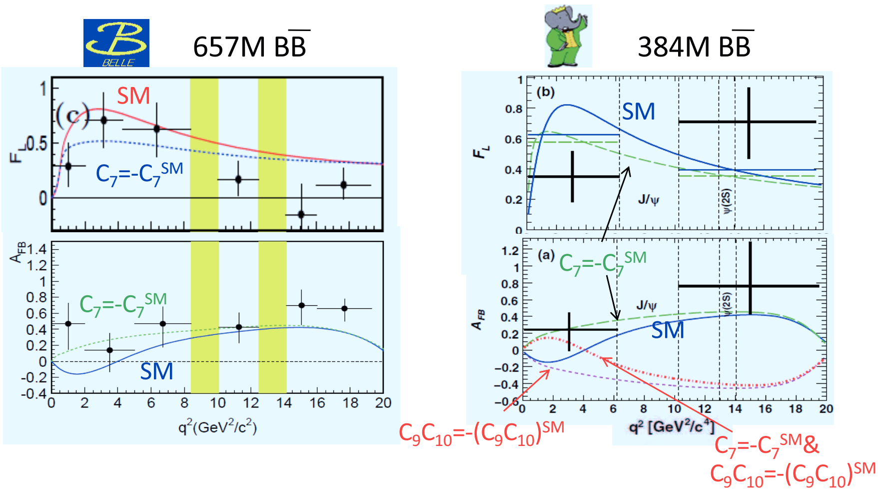

Figure 5: K^* longitudinal polarization fraction (F_L) and forward-backward asymmetry of the leptons (A_{FB}) for $B \to K^*\ell\ell$ measured by Belle (left) and BaBar(right).

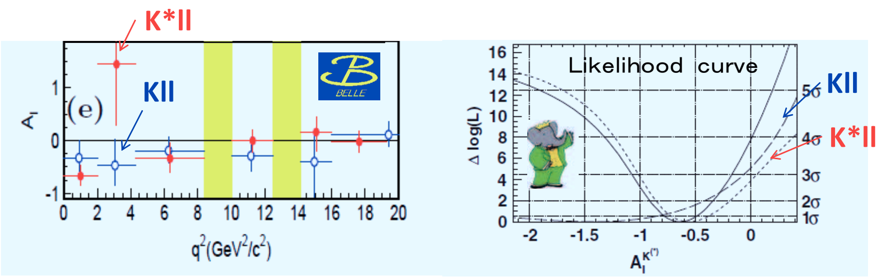

Figure 6: Isospin asymmetry (A_I) for $K^{(*)}\ell\ell$ measured by Belle (left) and BaBar(right).

The Belle collaboration has updated the result for the inclusive $B \to X_s\ell\ell$ process. The X_s system is reconstructed by one K^+ or K_S^0 plus up to four pions where number of π^0 is restricted to less than 1. The new results are obtained by using about 4 times more data and the improved background rejection than the previous measurement. Approximately, 240 decays are detected in the entire X_s mass region, and 56 decays in the mass region above K^*. The inclusive branching fraction for the entire mass region is deduced to be $(3.33 \pm 0.80^{0.19}_{-0.24}) \times 10^{-6}$.

5 Leptonic B decay ($B_{s(d)} \to \mu\mu$)

The leptonic B decays, $B_{s(d)} \to \mu\mu$, proceed via the diagrams shown in Figure 1-c). Within the SM, the branching fractions are predicted to be $O(10^{-9})$ for $B_s \to \mu\mu$ and $O(10^{-10})$ for $B_d \to \mu\mu$ [26]. The decay amplitude can be enhanced by several orders of magnitude in some SUSY models through the neutral Higgs exchange if the value of tanβ is large.

Figure 7 shows the result updated by CDF with 3.7 fb^{-1} data, based on analysis technique identical to the previous one with 2 fb^{-1} data. No significant excess are seen, and upper limits at 95%C.L. are found to be 4.3×10^{-8} for B_s and 7.6×10^{-9} for B_d [27]. The D0 collaboration has reported the expected upper limit using 5 fb^{-1} data, 4.7×10^{-8} for B_s at 95% C.L., that is similar to the limited obtained by CDF [28].

The present upper limits from CDF and D0 are about 10 times above the SM prediction. By accumulating more data; 6 fb^{-1} already at hand, and two times more data expected by the end of the Tevatron Run-II, and also by improving the analysis, they will provide significantly tighter constraints on NP parameter space.

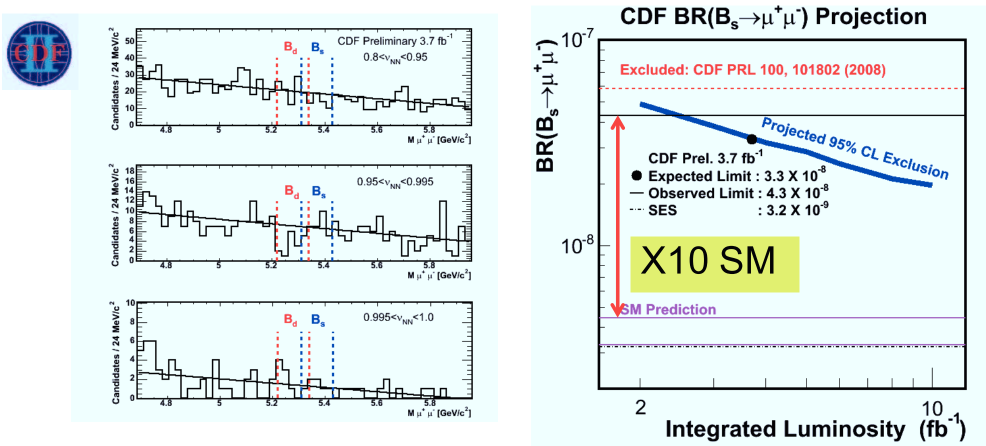

Figure 7: The di-muon invariant mass distribution in 3 NN(Neural Net) bins (left). Projected 95% C.L. exclusion limit as a function of the integrated luminosity (right).

6 Charmless Hadronic Decays

Charmless hadronic decays proceed via $b \to s$ gluonic penguin and/or $b \to u$ tree diagrams. The interference between the two diagrams induce direct CP violation. $B^+ \to \eta K^+$, $B^0 \to \rho^+\pi^-$, $B^+ \to \rho^0 K^+$, $B^+ \to D^{(*)0}K^+$.

6.1 $A_{CP}(K\pi)$ puzzle

The large luminosity data from the B factories have enabled us to measure the direct CP asymmetry (A_{CP}) for many charmless hadronic decay modes. Figure 8-a) summarizes the current status [3]. Up to now, direct CP violation has been observed in $K\pi$ and $\pi\pi$ decays, and evidence have been seen in 5 decay modes; $B^0 \to \eta K^{*0}$, The present average value for the

$B \to K\pi$ decay is $A_{CP}(K^+\pi^-) = -0.098^{+0.012}_{-0.011}$ and $A_{CP}(K^+\pi^0) = +0.050 \pm 0.025$, leading to the difference,

$$\Delta A_{CP}(K\pi) = A_{CP}(K^+\pi^0) - A_{CP}(K^+\pi^-) = 0.144 \pm 0.029\ . \qquad (4)$$

The difference is more than 5 σ significant, therefore, very firm experimentally. On the other hand, since the charged B decay amplitude must be similar to the neutral B, up to sub-leading corrections, one expect $\Delta A_{CP}(K\pi) \sim 0$. The sub-leading corrections may arise from electroweak penguin amplitude and color-suppressed tree amplitude. Enhancement of the color-suppressed tree amplitude may change $\Delta A_{K\pi}$, however, it would have to be larger than the color-allowed tree amplitude [29]. The electroweak amplitude could be the source of difference. However, as a loop amplitude, it can pick up a CP violating phase from NP. In order to clarify the issue, one can test the isospin relation between $A_{K\pi}$ asymmetry for the four $K\pi$ decays, $A_{K^-\pi^+}, A_{K^-\pi^0}, A_{K^0\pi^+}$ and $A_{K^0\pi^0}$ [30]. If the isospin relation violates, it would indicates that contribution of the electroweak penguin was significant. This require even more data because of the lower detection efficiency of $B^0 \to K^0\pi^0$, and also the necessity of flavor tagging to measure $A_{K^0\pi^0}$.

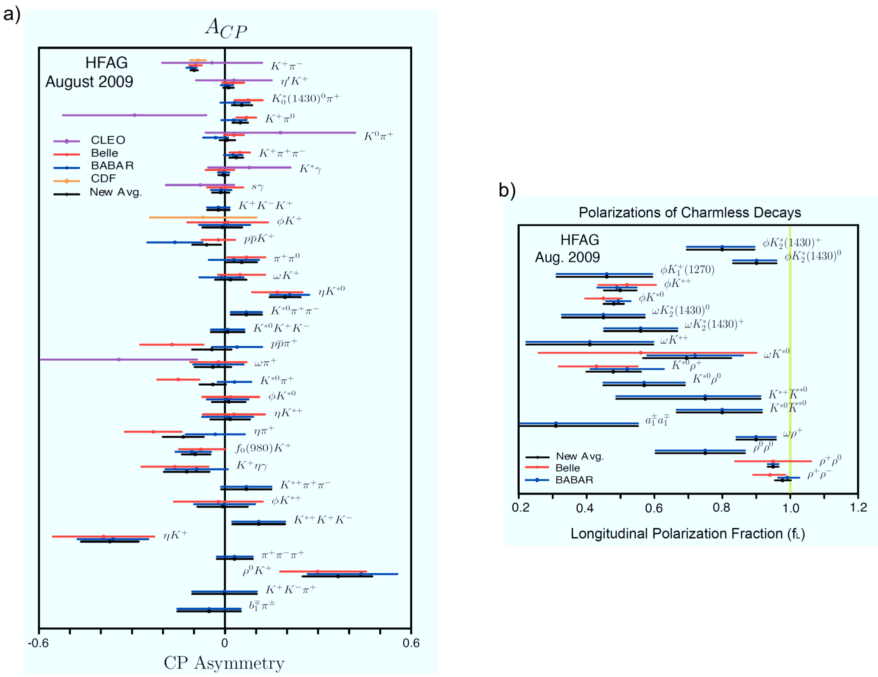

Figure 8: Current status of a) direct CP asymmetry and b) longitudinal polarization fraction in charmless hadronic B decays.

6.2 Modes including η and η'

The decay modes including η and η' have attracted much interests, since unexpectedly large branching fraction was measured at the CLEO experiment [31]. The BaBar collaboration has published updates for many decay modes including η and $\eta^{'}$, using the full data set, and found evidence for CP asymmetry $A_{CP}(B^+ \to \eta K^+) = -0.36 \pm 0.11 \pm 0.03$, and evidence for the three decay modes; $B^0 \to \eta K^0, \eta\omega$, and $\eta^{'}\omega$ [32]. The Belle collaboration has reported inclusive branching fraction for $B \to X_s\eta$, based on the 657M $B\bar{B}$ sample. The partial branching fraction for the X_s mass region from 0.4 to 2.6 GeV/c^2 is found to be $\mathcal{B}(B \to X_s\eta; 0.4 < M_{X_s}(\mathrm{GeV}/c^2) < 2.6) = (25.5 \pm 2.7 \pm 1.6^{+3.8}_{-14.2}) \times 10^{-5}$, where the last error is the modeling error [33].

6.3 $B \to VV$ modes

In the B meson decays to two vector mesons, $B \to VV$, we naively expect the longitudinal polarization factor is close to 1. However, the polarization factor for the penguin dominated $B \to \phi K^*$ decay was found to be about 0.5. Since then this problem has been known as the "polarization puzzle". On the other hand, the factor is close to one for the tree-dominated $B \to \rho\rho$ decay, and the vector-tensor decay mode $B \to \phi K_2^*(1430)$.

Improved understanding of these effects can come from data in decays such as $B \to \omega K^*$, which is related to $B \to \phi K^*$ via $SU(3)$ symmetry. The BaBar collaboration has reported measurements of B meson decays to the final states ωK^*, $\omega\rho$, and ωf_0, where K^* indicates a spin 0, 1 or 2 strange meson. The measured f_L is found to be near 1.0 for $B^+ \to \omega\rho^+$, as it is for $B \to \rho\rho$. On the other hand, for the vector-tensor $B\omega K_2^*(1430)$ decays, f_L is close to 0.5, as it is for $B \to \phi K^*$ decays, and about 4σ away from 1.0 for both charge states. They also measured the $b \to d$ penguin decays $B \to K^{*0}K^{*+}$ and its polarization [34].

7 Summary

In summary, the following points are addressed.

- The large data samples of B decays accumulated at the B experiments, Belle and BaBar, as well as the Tevatron experiments, CDF and D0, have made it possible to measure not only the branching fractions but also more detailed information (q^2 distribution, A_{CP}, A_{FB} etc. of rare B decays to probe NP.

- There are some hints of NP (puzzles) in the existing data; 1) $\mathcal{B}(B^- \to \tau^-\nu)$ larger than the prediction from the CKM fit, 2) $A_{FB}(B \to K^*\ell\ell)$ and $A_I(B \to K^*\ell\ell)$ in the low q^2 region deviated from the SM prediction, 3) Difference of CP asymmetry in $B \to K\pi$ decays between neutral and charged B decays, 4) Longitudinal polarization in $B \to VV$ decays smaller than the prediction.

- Search for $B_{s(d)} \to \mu\mu$ at Tevatron will be at critical corner in coming years.

- We need much more luminosity to clearly see the NP effects as the level of O(0.1) correction to the SM.

In the near future, more results with improved precision are expected from the B factories and the Tevatron experiments. Moreover, the next generation experiments, LHCb and Super B factories, will enable us measurements with much more improved precision. Let us prepare for exciting future in B physics !

Acknowledgments

This work is supported in part by a Grant-in-Aid for Scientific Research on Priority Areas "New Developments of Flavor Physics" from the ministry of Education, Culture, Sports, Science and Technology of Japan.

References

[1] M. Kobayashi and T. Maskawa, Prog. Theor. Phys. **49**, 652 (1973).

[2] C. Amsler *et al.*(Particle Data Group), Phys. Lett. B **667**, 1 (2008).

[3] The average at ICHEP2008 calculated by the Heavy Flavor Averaging Group, http://www.slac.stanford.edu/xorg/hfag/semi/index.html

[4] Elvira Gamiz, Christine T. H. Davies, G. Peter Lepage, Junko Shigemitsu, Matthew Wingate, Phys. Rev. D **80**, 014503 (2009).

[5] W. S. Hou, Phys. Rev. D **48**, 2342 (1993).

[6] K. Ikado *et al.* (Belle Collaboration), Phy. Rev. Lett. **97** 251802 (2006).

[7] I. Adachi *et al.* (Belle Collaboration), arXiv:0809.3834.

[8] B. Aubert *et al.* (BaBar Collaboration), Phys. Rev. D **77**, 011107(R) (2008).

[9] B. Aubert *et al.* (BaBar Collaboration), arXiv:0809.4027.

[10] C.-H. Chen and C.-Q. Geng, J. High Energy Phys. 10, 053 (2006).

[11] B. Grzadkowski and W.-S. Hou, Phys. Lett. B **283**, 427 (1992); M. Tanaka, Z. Phys. C **67**, 321 (1995); K. Kiers and A. Soni, Phys. Rev. D **56**, 5786 (1997); H. Itoh, S. Komine and Y. Okada, Prog. Theor. Phys. **114**, 179 (2005); Ulrich Nierste, Stephanie Trine, Susanne Wesoff, arXiv:0801.4938.

[12] B. Aubert *et al.* (BaBar Collaboration), Phys. Rev. Lett. **100**, 021801 (2008); Phys. Rev. D **79**, 092002 (2009).

[13] A. Matyja, M. Rozanska *et al.* (Belle Collaboration), Phys. Rev. Lett. **99**, 191807 (2007).

[14] I. Adachi *et al.* (Belle Collaboration), arXiv:0910.4301.

[15] B. Aubert *et al.* (BaBar Collaboration), Phys. Rev. D **79**, 091101(R) (2009).

[16] B. Aubert *et al.* (BaBar Collaboration), Phys. Rev. D **80**, 111105(R) (2009).

[17] B. Aubert *et al.* (BaBar Collaboration), Phys. Rev. Lett. **103**, 211802 (2009).

[18] B. Aubert *et al.* (BaBar Collaboration), Phys. Rev. D **79**, 011102(R) (2009).

[19] R. Wedd *et al.* (Belle Collaboration), arXiv:0810.0804, to appear in Phys. Rev. D (RC).

[20] I. Adachi *et al.* (Belle Collaboration), arXiv:0911.1779.

[21] A. Limosani *et al.* (Belle Collaboration), Phys. Rev. Lett. **103**, 241801 (2009).

[22] M. Misiak *et al.*, Phys. Rev. Lett. **98**, 022002 (2007).

[23] J.-T. Wei, P. Chang *et al.* (Belle Collaboration), Phys. Rev. Lett. **103**, 171801 (2009).

[24] B. Aubert *et al.* (BaBar Collaboration), Phys. Rev. D **79**, 031102(R) (2009); B. Aubert *et al.* (BaBar Collaboration), Phys. Rev. D **73**, 092001 (2009).

[25] T. Aaltonen *et al.* (CDF Collaboration), Phys. Rev. D **79**, 011104(R) (2009).

[26] A.J. Buras, Phys. Lett. B **566**, 115 (2003).

[27] See http://www-cdf.fnal.gov/physics/S09CDFResults.html.

[28] D0 Note 5906-CONF.

[29] S. Baek and D. London, Phys. Lett. B **653**, 249 (2007); S. Baek *et al.* Phys. Rev. D **71**, 057502 (2005).

[30] M. Gronau and J. Rosner, Phys. Rev. D **74**, 057503 (2006).

[31] T.E. Browder *et al.* (CLEO Collaboration) Phys. Rev. Lett. **81**, 1786 (1998); G. Bonvicini *et al.* (CLEO Collaboration) Phys. Rev. D **68**, 011101 (2003).

[32] B. Aubert *et al.* (BaBar Collaboration), Phys. Rev. D **80**, 112002 (2009).

[33] I. Adachi *et al.* (Belle Collaboration), arXiv:0910.4751.

[34] B. Aubert *et al.* (BaBar Collaboration), Phys. Rev. D **79**, 052005 (2009).

Discussion

Achmed Ali (DESY): Your data seem to show some deviations in $K^* \rightarrow l^+l^-$ forward backward asymmetry and in the isospin asymmetry, but you did not show us the di-lepton mass spectrum itself. How does this spectrum compare to the existing models you have?
Answer: The dilepton mass spectrum is shown in the slide, and is consistent with the Standard Model within uncertainties.